AD_____

Award Number: W81XWH-07-1-0579

TITLE: Development of a Novel Tissue Engineering Strategy Towards Whole Limb Regeneration

PRINCIPAL INVESTIGATOR: Cato T. Laurencin, M.D., Ph.D.

CONTRACTING ORGANIZATION: University of Virginia
Charlottesville, VA 22904

REPORT DATE: August 2008

TYPE OF REPORT: Final

PREPARED FOR: U.S. Army Medical Research and Materiel Command
Fort Detrick, Maryland 21702-5012

REPORT DOCUMENTATION PAGE

Form Approved
OMB No. 0704-0188

1. REPORT DATE	2. REPORT TYPE	3. DATES COVERED
17-08-2008	Final	18 JUL 2007 - 17 JUL 2008

4. TITLE AND SUBTITLE

Development of a Novel Tissue Engineering Strategy Towards Whole Limb Regeneration

5a. CONTRACT NUMBER

5b. GRANT NUMBER
W81XWH-07-1-0579

5c. PROGRAM ELEMENT NUMBER

6. AUTHOR(S)
Cato T. Laurencin, M.D., Ph.D.

Email: ctl3f@virginia.edu

5d. PROJECT NUMBER

5e. TASK NUMBER

5f. WORK UNIT NUMBER

7. PERFORMING ORGANIZATION NAME(S) AND ADDRESS(ES)

University of Virginia
Charlottesville, VA 22904

8. PERFORMING ORGANIZATION REPORT NUMBER

9. SPONSORING / MONITORING AGENCY NAME(S) AND ADDRESS(ES)
U.S. Army Medical Research and Materiel Command
Fort Detrick, Maryland 21702-5012

10. SPONSOR/MONITOR'S ACRONYM(S)

11. SPONSOR/MONITOR'S REPORT NUMBER(S)

12. DISTRIBUTION / AVAILABILITY STATEMENT
Approved for Public Release; Distribution Unlimited

13. SUPPLEMENTARY NOTES

14. ABSTRACT

Tissue engineering has been a highly successful strategy for regenerating individual musculoskeletal tissue types, and holds great potential as a strategy for whole limb regeneration. In contrast to the bottom up approach of limb regeneration that relies on blastema formation, outgrowth, and cell dedifferentiation as seen in amphibians and lower vertebrates, tissue engineering utilizes a top down approach that integrates material science, cell and molecular biology, and engineering. The aim of this research program is to take full advantage of this new direction to develop novel tissue engineering strategies for regenerating whole limbs in mammalian models. The tasks we have proposed use the collective expertise and insights of the group to test the hypothesis that functional organs can be regenerated by actively integrating the individual component tissues developed via the tissue engineering approach through the administration of appropriate environmental cues for limb regeneration. Key findings of this research program include the successful formation of both microspherebased, nanofiber-based, and composite microsphere-nanofiber structures for bone, cartilage, and ligament, growth factor binding to and release from scaffolds, cellular evaluation of marrow-derived, mesenchymal, and cell-specific cells on scaffolds, in vivo visualization of vascularization of composite scaffolds, and in vivo biocompatibility studies of scaffolds.

15. SUBJECT TERMS
Tissue engineering, musculoskeletal, scaffolds, bioresorbable, growth factors, stem cells, translational research

16. SECURITY CLASSIFICATION OF:			17. LIMITATION OF ABSTRACT	18. NUMBER OF PAGES	19a. NAME OF RESPONSIBLE PERSON
a. REPORT	b. ABSTRACT	c. THIS PAGE			19b. TELEPHONE NUMBER *(include area code)*
U	U	U	UU	19	USAMRMC

Table of Contents

INTRODUCTION

Tissue engineering has been a highly successful strategy for regenerating individual musculoskeletal tissue types, and holds great potential as a strategy for whole limb regeneration. In contrast to the bottom up approach of limb regeneration that relies on blastema formation, outgrowth, and cell dedifferentiation as seen in amphibians and lower vertebrates, tissue engineering utilizes a top down approach that integrates material science, cell and molecular biology, and engineering. The aim of this research program is to take full advantage of this new direction to develop novel tissue engineering strategies for regenerating whole limbs in mammalian models.

We have accumulated substantial preliminary data from our collaborations using the tissue engineering approach to regenerate the individual constituent tissues of the musculoskeletal system. The tasks we have proposed use the collective expertise and insights of the group to test the hypothesis that functional organs can be regenerated by actively integrating the individual component tissues developed via the tissue engineering approach through the administration of appropriate environmental cues for limb regeneration.

As a first step we will develop integrated graft systems (IGS) such as osteochondral, osteoligamentous, and vascularized tissues (Task I). Subsequent steps will examine the integration of peripheral nerve into other tissue systems and to develop additional component tissues such as skin and tendon (Task II). Final steps include regenerating whole joints using rabbit and dog models, and to investigate the early translation of our paradigms using human cells. (Task III and IV)

The military implications of the proposed work are particularly evident from the increasing incidence of amputations from battlefield injuries. The need to regenerate limbs and restore the functional capacity and quality of life of these otherwise healthy individuals is of central importance to the project. It is the opinion of the PI and assembled team that a top down approach utilizing tissue engineering as a platform shows the greatest promise for success in this challenge, and the previous accomplishments and collective expertise of the PI and assembled team maximize the likelihood of success.

BODY

QUARTER 1

The following milestones were identified within the first quarter:

Matrix Studies

-Spin nanofibers on microsphere matrices
-Melt (with heat or solvent) nanofiber mesh onto sintered microsphere matrices
-Evaluate strength of interface through tensile testing
-BMP-2 delivery from microsphere matrices using 3 different concentrations
-Protein delivery (bovine serum albumin) from nanofiber matrices

Cell Studies

-Isolation of rabbit mesenchymal stem cells, adipose-derived stem cells, osteoblasts, and chondrocytes
-Seeding of cells on matrices and evaluation of cellular differentiation
    -Osteoblast markers: alkaline phosphatase, osteocalcin, osteopontin, alizarin red, type I collagen
    -Chondrocyte markers: safranin O, type II collagen
    -Mechanical properties of cartilage assessed after 4-6 weeks of culture using compression testing

Below is a summary of findings and accomplishments according to the above objectives:

Incorporation of Nanofiber Meshes onto Microsphere Matrices through Spinning, Melt, and/or Solvent Bonding and Evaluation of Nanofiber-Microsphere Interfacial Strength

Studies have been conducted to evaluate different methods of bonding the interface between the microspheres (bone regeneration) and nanofibers (cartilage regeneration).

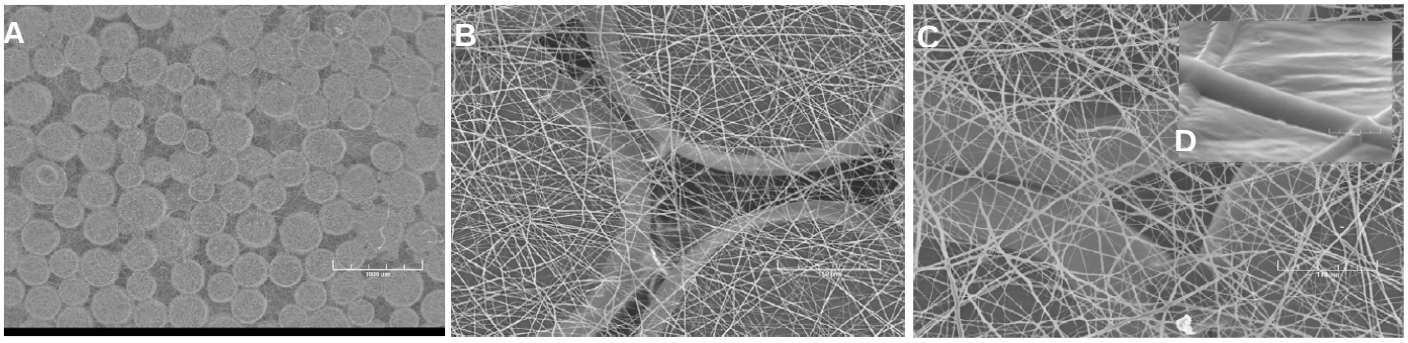

Figure 1. Nanofibers spun directly onto microsphere matrices. (A) Nanofibers can be seen coating a layer of microspheres. (B) Higher magnification SEM of nanospheres over microspheres. (C) Nanospheres can be seen embedded into the surface of the microspheres after 30 minutes of heating at

Three methods were evaluated: electrospinning fibers directly onto microspheres, using heat to sinter nanofibers to microspheres, and using solvent to bond nanofibers to microspheres. Figure 1A and 1B show scanning electron micrographs of the first approach, spinning fibers directly onto microspheres. Results indicated that the bond between nanofiber and microsphere was weak to non-existent when simply spun onto the surface. As an additional trial, nanofibers that were spun onto the surface of the microspheres were sintered to the surface of the microspheres after spinning by incubating the nanofiber/microsphere composite for 30 minutes at 60ºC, just above the glass transition temperature. Figure 1D shows the effect of the heating; the nanofiber becomes embedded into the surface of the microsphere without any deleterious effects on the nanofiber structure.

Although the nanofibers bonded with the microspheres the strength of the bond was very weak. As an alternative strategy, a combination of heat, solvent, and light pressure was used to bond the two interfaces. Acetone was applied to the nanofiber surface prior to bonding the two interfaces. After laying the nanofibers onto the microspheres, a 0.5 kg weight was applied to the two materials and it was placed in a 60ºC oven for 15 minutes. Results are shown in figure 2, in which the higher concentration of acetone resulted in a stronger bond between the two materials.

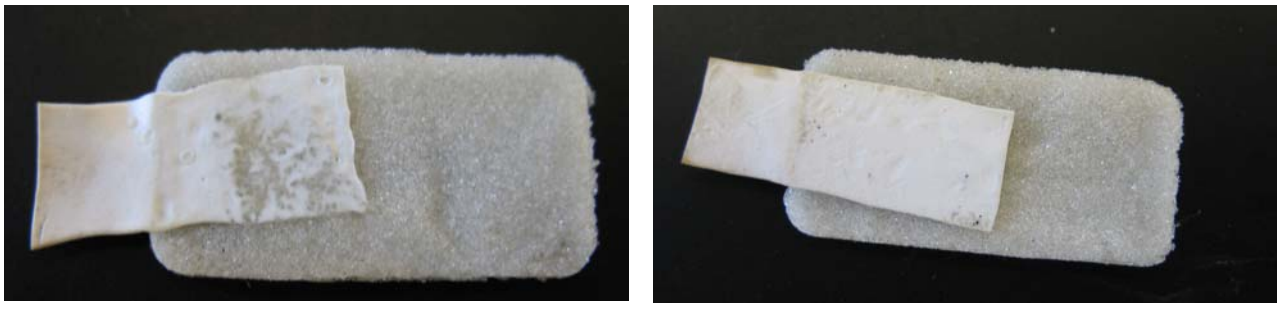

Figure 2. Combination of heat, pressure, and solvent used to bond nanofiber matrix to microsphere matrix to form the interface between chondral tissue and osseous tissue. (A) Mixture of acetone:H_2O at a ratio of 2:3 and (B) mixture of acetone:H_2O at a ratio of 1:4. Higher concentration of acetone in (A) yields a stronger bond between the two interfaces.

Mechanical testing of the interface between nanofibers and microspheres after applying heat and solvents to bond the two interfaces, showed the following results.

BMP-2 Loading and Delivery from Microsphere Matrices

Extensive evaluation of BMP-2 loading and delivery from microsphere matrices has been performed. Three separate loading concentrations were utilized and loaded onto composite microsphere matrices. Cylindrical scaffolds, 5mm X 5mm, were constructed by sintering microspheres of diameters ranging from 350-600 μm. Scaffolds with two different HA/PLAGA compositions were studied, HIGH (83% PLAGA) and LOW (73% PLAGA), according to their polymer/ceramic ratio. Control scaffolds of pure polymer, called PLAGA, were constructed in the same way as the composite scaffolds, except for the omission of aqueous HA precursor solutions. Protein was loaded by incubating the scaffolds with 30μl of 30μg/ml, 125 μg/ml, or 500 μg/ml rhBMP-2 (Genscript, city/state) in 5 mM glutamate buffer, pH 4.5 for 24 hrs.

FREE protein, or that which remained in the loading solution following BMP-2 adsorption, was quantified by collecting the loading solution via centrifugation and measuring the BMP-2 concentration via RP-HPLC. BOUND protein was defined as protein which was transferred from the BMP-2 loading solution to the scaffold and could not be separated from the graft via centrifugation. This group was calculated by subtracting the FREE protein from the total protein originally loaded. A sample size of three was used for all experiments, and 2-way ANOVA with Tukey test was used for statistical analysis.

Results of the BMP-2 loading experiments suggest that the HA-PLAGA scaffolds never became saturated with BMP-2, as nearly all of the rhBMP-2 in the 30μg/mL, 160μg/mL, and 813μg/mL solutions was transferred from FREE to BOUND upon incubation. The PLAGA scaffolds, however, seemed to become saturated with the BMP-2 at a loading solution concentration between 160ug/mL and 813ug/mL. Figure 3(a) shows the FREE protein associated with the PLAGA, HIGH, and LOW scaffolds loaded with 30μg/mL, 160μg/mL, and 813μg/mL BMP-2 solutions. The PLAGA scaffold loaded with 813μg/mL was the only graft that contained a substantial amount of FREE protein, with 22.32±1.59μg FREE BMP-2 loaded. The other scaffolds, including the HIGH and LOW composites

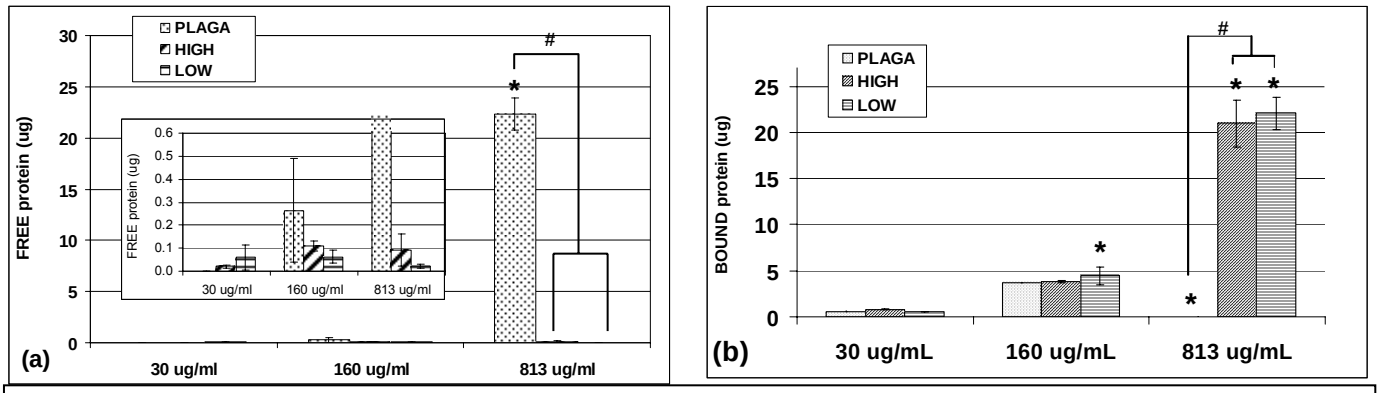

Figure 3 show the FREE (a) and BOUND (b) protein (μg) loaded onto the PLAGA, HIGH, and LOW scaffolds using 30μg/mL, 160μg/mL, and 813μg/mL BMP-2 loading solutions. Significance is designated with (*) for concentration within a single material and (#) for material within a single concentration, p≥0.05.

loaded with all three loading solution concentrations, and the PLAGA scaffolds loaded with 30µg/mL and 160µg/mL had less than 0.3ug FREE protein. Figure 3(b) shows the BOUND protein that was calculated as the difference between the total and FREE protein loaded on each scaffold. From this Figure, it is evident that nearly all of the BMP-2 loaded onto the HA-PLAGA composite scaffolds was in the form of BOUND protein. The PLAGA scaffolds loaded with 30ug/mL and 160ug/mL BMP-2 solutions also loaded nearly all of their protein as BOUND.

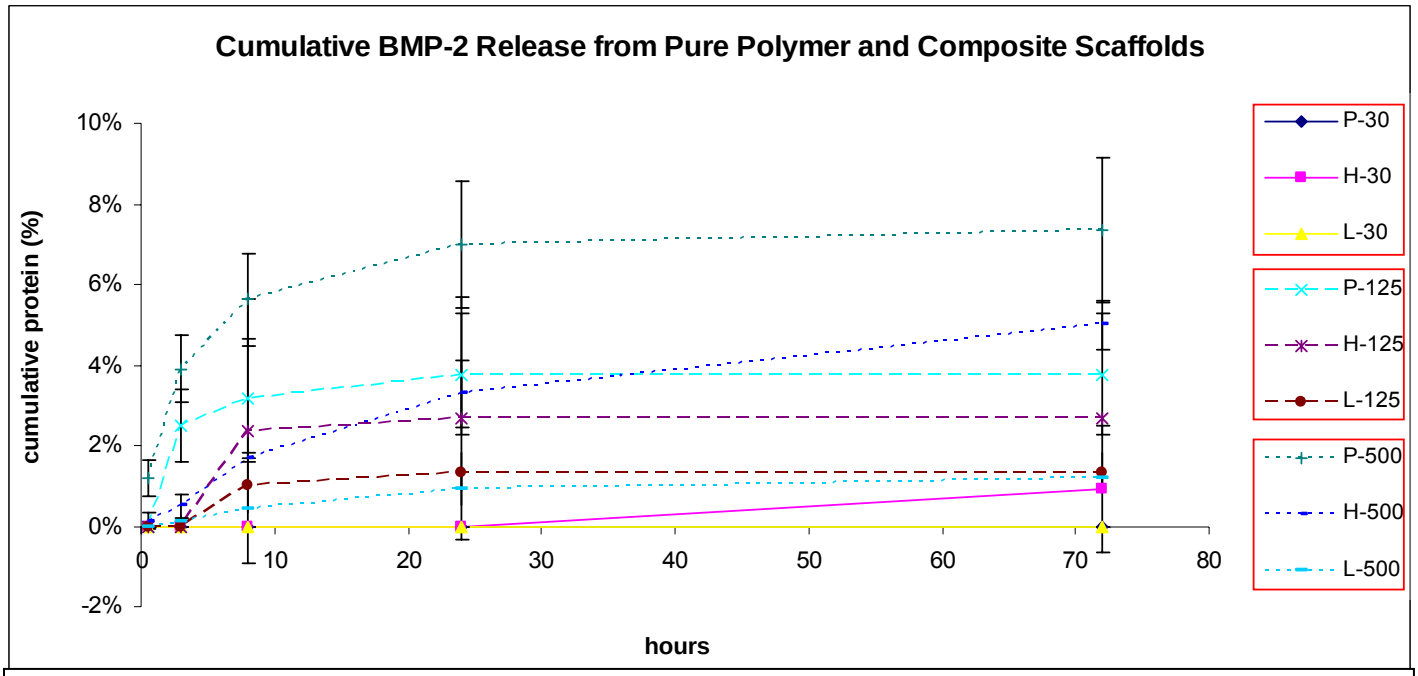

Figure 4. Cumulative release of BMP-2 from polymer and polymer/ceramic composite scaffolds over 3 days. Scaffolds containing calcium phosphate were found to deliver BMP-2 more gradually over a longer period of time, while higher protein loadings resulted in greater amounts of BMP-2 released.

The results of the BMP-2 loading studies show that the HA-PLAGA scaffolds have an increased capacity for protein adsorption. At the pH of the loading solution (pH 4.5), the negatively charged phosphate groups introduced by the HA strongly attracted the positively charged BMP-2, which has a pI of around 9. The ionic interaction between the BMP-2 and HA was more effective than that between the BMP-2 and carboxylic acid groups of PLAGA. Greater protein loading capacity could lead to a more sustained delivery of BMP-2 to local cells once the grafts are implanted, and result in a more efficient graft.

Release studies have been performed for the earliest time points up to 3 days. It can be seen from this data that amount of BMP-2 released is directly proportional to the amount of protein (30µg, 125µg, and 500µg). Additionally, it can be seen that pure polymeric scaffolds (indicated as P in the legend) and composite scaffolds with either a low (L) or a high (H) calcium phosphate content deliver the BMP-2 with varied kinetics. The absence of calcium phosphate results in more of a burst release (see curves for P-125 and P-500) but the presence of the ceramic results in a more sustained release over time and also a reduced release overall in the shortest time points (<3 days). These results suggest that the presence of calcium phosphate within the bone composite scaffolds may provide delivery kinetics of BMP-2 that may more suitably aid in the regeneration of bone,

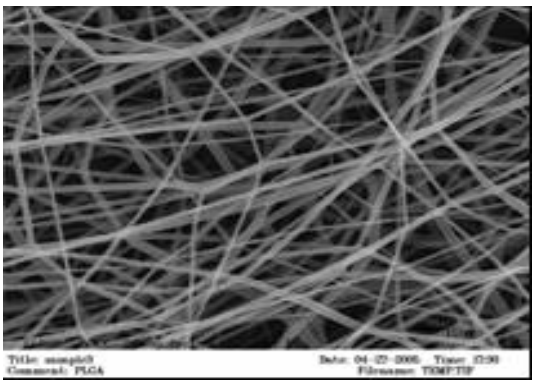

Figure 5. SEM of PLAGA nano fibers

or bony tissue.

BSA Delivery from Nanofiber Matrices

Early preliminary studies evaluating protein release from fibers revealed that release kinetics were faster than expected. Rather than evaluate the release of TGF-β, therefore, a more comprehensive evaluation of protein release was performed using bovine serum albumin as a vehicle rather than the growth factor. Results are as follows:

Nanofiber Fabrication: The nanofibers were fabricated via electrospinning (see figure 5). A polymer concentration > 20% (w/v) in an admixture of solvent (75% tetrahydrofuran (THF) and 25% dimethyl formamide (DMF)) at a constant at flow rate of 2mL/h, applied electrical potential of 30kV, working distance 30cm, and with 20 needle gauge resulted in the formation of nanoscale fibers from PLAGA with a LA/GA (lactic acid/glycolic acid) ratio of 50:50.

Nanofiber and microfiber Characterization: Nanofiber morphology was determined by scanning electron microscopy (SEM). Figure 5 shows the SEM of PLAGA nanofibers formed by the optimized process. The *in vitro* degradation of the nanofibers was performed in Dulbecco minimal Eagle medium (DMEM) at 37°C and was followed for 2 weeks. The nanofibers were found to show significant decrease in molecular weight during the 14 day degradation time.

Protein Encapsulation: We attempted to encapsulate PLAGA nanofibers with bovine serum albumin, having molecular weight in the range of the growth factor we propose to load in the nanofibers, TGF-β. Thus 3 different concentrations of protein were encapsulated with two different polymer concentrations. Protein encapsulation was carried out with respect to the dry weight of polymer. In a typical loading 20% of PLAGA (50:50) solution was prepared by dissolving 2g of polymer in 10ml of solvent (THF:DMF) in a ratio of 3:1. Calculated amount of protein was dissolved in 400µL of deionized water. This protein solution was added drop wise slowly without any visual precipitation by gentle shaking. The polymer protein solution was sonicated for 10 min to ensure complete mixing of protein and breakdown of water droplets size. This solution was filled in 10 ml glass syringe and set for electrospinning. The protein encapsulation and spinning details are as shown in the table. The samples were dried for 24 hours in vacuum at room temperature and stored in polyethylene bags and kept under vacuum until further use.

To measure the amount of protein encapsulated within the nanofiber matrix, a known amount of protein loaded nanofiber mat was taken in a test tube with predetermined quantity of water. The suspension was allowed stay for a week at 37°C and then the tube was sonicated for 1 hr to enhance the release and all the bound protein is released into the water. This solution was analyzed using HPLC (Agilent). We have developed a suitable HPLC method to assay these three proteins. The HPLC method details are as follows:

Column Name: PRP-3 Reversed Phase
Conditions: solvent A) 0.1% TFA in Water pH 2.0 solvent B) 0.1% TFA in Acetonitrile.
Linear gradient 15-60% in 6 min. Ambient
Flow rate: 2 mL/min,
Injection: 100µL
Detection: UV at 215 nm
Encapsulation efficiency was calculated by using:
Encapsulation Efficiency = (Experimentally found concentration) / Theoretical Loading X 100

A systematic trend was observed in terms of the encapsulation efficiency of the protein studied. With increasing polymer concentration encapsulation efficiency increased. This may be due to the

increase in the diameters of the nanofibers formed at higher polymer concentration. Also it has been found that with decrease in % loading of protein, encapsulation efficiency increased.

Table 1 shows the encapsulation efficiency of the BSA in PLAGA nanofibers developed under the optimized spinning conditions.

TABLE 1: Bovine Serum Albumin Encapsulation efficiency

PLGA Concentration	Needle Gauge	Flow rate	Working Distance	Applied Voltage	BSA Loading	Encapsulation Efficiency
20%	18	1mL	30 cm	30 kV	2.5%	87 %
25%	18	1mL	30 cm	30 kV	2.5%	90 %
20%	18	1mL	30 cm	30 kV	1.5%	89 %
25%	18	1mL	30 cm	30 kV	1.5%	92%
20%	18	1mL	30 cm	30 kV	0.5%	92%
25%	18	1mL	30 cm	30 kV	0.5%	93%

Figure 6A shows the SEM of PLAGA nanofibers loaded with BSA under the conditions described above. Figure 6B shows the SEM of BSA loaded nanofibers after the release of BSA into phosphate buffer at 37°C for 8 days. The fibers loaded with BSA released 60%-70% of the BSA within 30 minutes of incubation, and was followed by a more sustained release for the following 10 days. The fibers themselves, however, were found to have been degraded considerably after 8 days of incubation in PBS. Due to the challenges associated with the pre-loading techniques such as difficulties in loading higher concentration of the proteins and altered degradation pattern of the matrices due to the incorporation of aqueous protein solution, a post-loading technique was recently optimized to load bioactive factors in the nanofiber matrices. In post loading the nanofiber matrices in appropriate size will be incubated in different concentrations of the bioactive factors such as (TGF-β) [1-100 ng/ml]. The release of the loaded factors is currently being evaluated using high performance liquid chromatography and Enzyme-Linked Immuno Sorbent Assay (ELISA) assay methods.

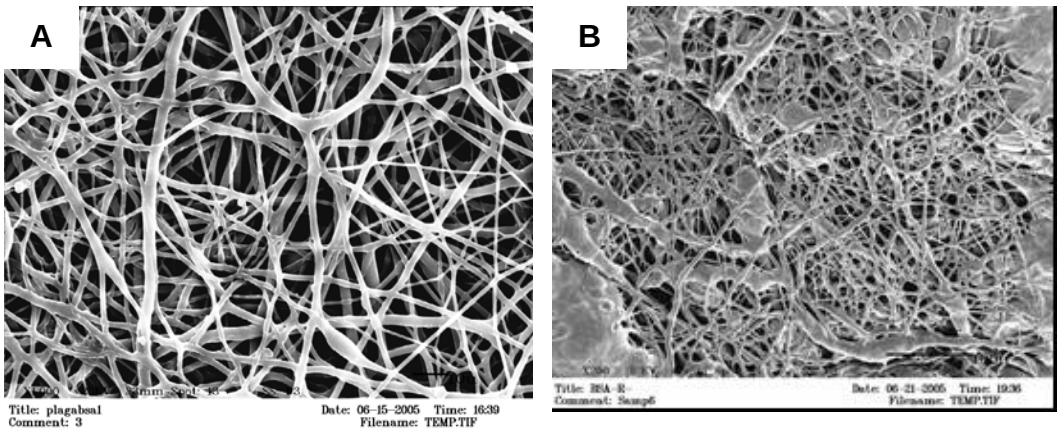

Figure 6. SEM showing the morphology of BSA loaded nanofibers before (A) and after (B) *in vitro* release in PBS.

Cellular Evaluation of Microsphere Matrices

Rabbit Bone Marrow Stromal Cells on PLAGA-HA Composite Microsphere Matrices

To evaluate the efficacy of composite microsphere matrices supporting cellular growth, proliferation, and differentiation, rabbit mesenchymal stem cells were isolated with bone marrow stromal cells and seeded onto matrices. Cells were isolated, plated, and passaged 4-5 times prior to seeding onto scaffolds. Once cells reached P4-5, cells were trypsinized and seeded onto scaffolds at a concentration of 50,000 cells/scaffold, which were formed into cylinders measuring 2.5mm high x 4 mm in diameter. Cells on scaffolds were incubated for 7, 14, and 21 days during which they were evaluated for proliferation, alkaline phosphatase expression, and mineralization. Results indicated that cells proliferated on matrices over the 21 day evaluation, but also showed both qualitative

(through staining) and quantitative increases for alkaline phosphatase and alizarin red. This data suggests that undifferentiated progenitor cells, when seeded on composite scaffolds, express phenotypic markers specific for osteoblasts and also produce mineral.

Figure 7. Cell proliferation, alkaline phosphatase expression, alkaline phosphatase staining, and mineralization of marrow derived stem cells on composite matrices, indicating normal phenotypic expression of seeded osteoblasts.

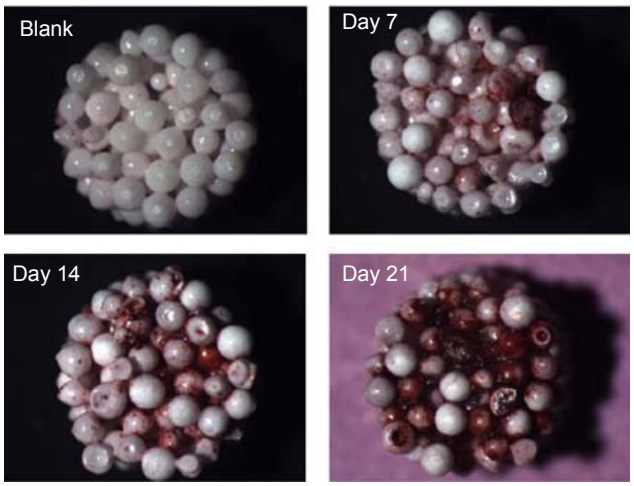

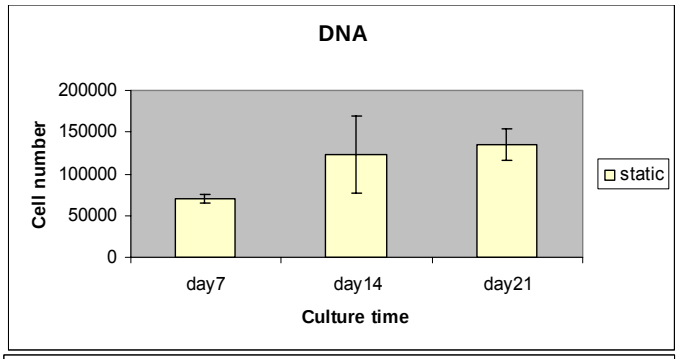

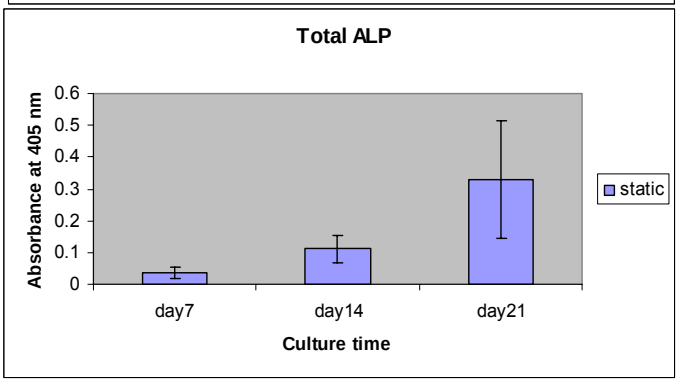

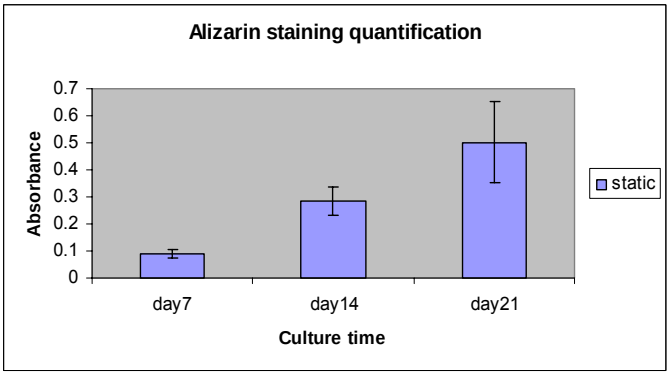

Cellular Evaluation of Nanofiber Matrices

Isolation of chondrocytes and proliferation.

Briefly, 1g of rib cartilage was harvested aseptically from a male New Zealand white rabbit (weighing 3.5–4.5 kg). The cartilage was diced and digested in 0.1% (weight/volume) collagenase type II (Worthington, Freehold, HJ) for 3 to 6 h at 37ºC to release the chondrocytes. The harvested chondrocytes were then resuspended in Dulbecco's Modified Eagle's Medium (DMEM) containing 4.5 gm/l glucose, 10% fetal bovine serum, 50 mg/l sodium ascorbate, 10mM HEPES, 100 units/ml penicillin, and 100 mg/ml streptomycin. Primary chondrocytes were plated in two to three T-75 cm^2 flasks at 1×10^5 cells/cm^2 and cultured in a humidified, 5% CO_2 incubator for 5 to 7 days. Second passage chondrocytes were used throughout the experiment.

Culture of rabbit chondrocytes on the poly (lactide-*co*-glycolide)(50:50) nanofiber scaffold

PLGA nanofiber scaffolds were cut into strips measuring 5mm×40mm, and pre-soaked with 70% ethanol for 3min to minimize the likelihood of bacterial contamination during culture. The ethanol was then exchanged for an excess amount of PBS, after which the strips were sterilized under ultraviolet light for 1h. A chondrocyte cell suspension (approximately 5×10^5 cells/strip) was seeded onto the strips, then cultured for 1 h prior to the addition of culture medium (Dulbecco's Modified Eagle's Medium) (DMEM) into the dish. The culture medium contained 4.5 gm/l glucose, 10% fetal bovine serum, 50 mg/l sodium ascorbate, 10mM HEPES, 100 units/ml penicillin, and 100 mg/ml streptomycin.

Safranin-O staining and type II collagen immunostaining

The histology of the construct was evaluated microscopically on sections that had been stained with 0.1% Safranin-O (Sigma). Type II collagen was immunolocalized in the construct as follows. Freshly harvested samples were preserved in Optimal Cutting Temperature Compound (Sakura, Torrance, CA), and 10 mm sections were prepared using a Leica CM3050 cryomicrotome (Leica, Bannockburn, IL) at -30ºC. Sections were incubated with mouse monoclonal anti-type II collagen (Sigma), followed by fluorescein isothiocyanate (FITC) labeled goat anti-mice IgG (American Qualex, San Clemente, CA). Fluorescence was visualized with a Nikon Eclipse E600 microscope (Nikon, Melville, NY) equipped with a digital camera and images were analyzed using the Adobe Photoshop 7.0 software (Adobe system Incorporated, San Jose, CA).

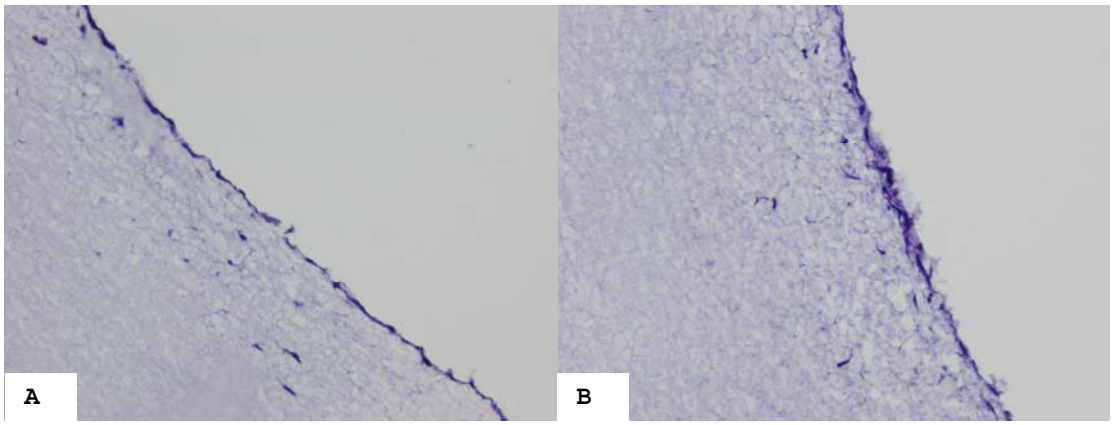

Figure 8. Safranin-O staining after the rabbit chondrocytes were cultured in the scaffold for 1 week (A) and 2w (B). (200X)

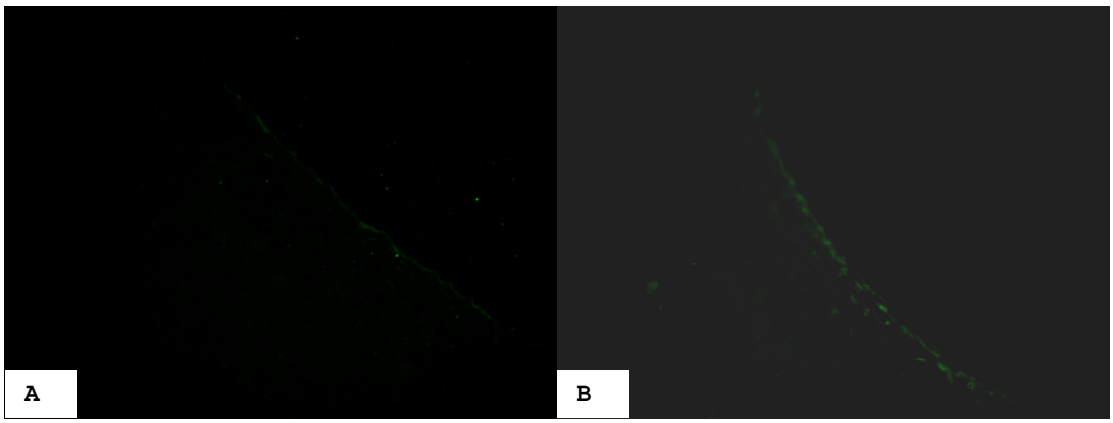

Figure 9. Immunostaining of type II collagen staining after the rabbit chondrocytes were cultured in the scaffold for 1 week (A) and 2w (B).

The rabbit chondrocytes were seeded onto the PLGA nanofiber scaffold and cultured for 1 to 2 weeks. The scaffold supported growth of the rabbit chondrocytes as seen in figure 8 along the seeded border of the nanofiber mesh. The cells on the scaffold proliferated and had achieved complete confluence after 2 weeks in culture. In addition, the rabbit chondrocytes produced proteoglycan (Fig. 8) and type II collagen (Fig. 9), which are the major extracellular matrix components of chondrocytes. These findings demonstrated the rabbit chondrocytes could maintain its phenotype on PLGA nanofiber. It was also noted, however, that the nanofiber degraded considerably over the two-week culture period, suggesting the use of 85:15 may be more suitable to the task at hand.

At the completion of Quarter 1 we have established the following:
The bonding between the nanofiber and microsphere matrices to form the osteochondral interface was achieved through the use of a combination of heat, solvent of appropriate strength, and light pressure. Spinning the nanofibers directly onto the surface of the microspheres, although possible, resulted in a very weak bond between the two interfaces.

BMP-2 protein loading and delivery from microsphere matrices was found to be dependent on the concentration of protein in solution, and was also found to be enhanced through the addition of calcium phosphate to the matrix via composite microsphere formation.

Protein delivery from nanofibers was found to be challenging as BSA was released from nanofibers within 30 minutes of PBS incubation. This preliminary study was performed in lieu of the proposed TGF-β for precisely this reason; to evaluate the rough kinetics of delivery. Work is ongoing to slow the rate of release of BSA from nanofibers. Once kinetics approximating those desired are achieved, TGF-β release from nanofibers will be evaluated.

Rabbit marrow cells seeded on microsphere matrices with calcium phosphate were found to show proliferation, alkaline phosphatase expression, and mineralization increases over time, suggesting that the microsphere matrix is capable of supporting and potentially differentiating rabbit marrow-derived stem cells over time. Adipose-derived stem cells will be evaluated subsequently, as will rabbit osteoblasts.

Chondrocytes isolated from rabbit cartilage were found to proliferate and maintain their phenotype (as evidenced by safranin-O staining) and begin to form a type II collagen extracellular matrix (as evidenced by positive type II collagen staining). It was also determined that 50:50 PLAGA may not be suitable for cartilage as the degradation time is very short. 85:15 PLAGA will be evaluated subsequently.

QUARTER 2
The following milestones were identified within the second quarter:

Matrix Studies
-Synthesize and integrate braided ligament structures with microsphere matrices
    -Melt braided fibers onto end of microsphere matrix using solvent or heat
    -Integrate braided fibers within loose microspheres prior to sintering
-Evaluate interface strength via tensile testing and compare to native bone-ligament interface strength
-Evaluate pore volume and pore diameter of integrated constructs

Cell Studies
-Isolation of rabbit patellar tendon cells
-Seeding of tendon cells on matrices and evaluation of cellular differentiation

Below is a summary of findings and accomplishments according to the above objectives:

<u>Synthesis and integration of braided ligament structures with microsphere matrices</u>
To synthesize the braided ligament, a 64-carrier 3-dimensional braiding machine was used. Specifically, a single 70 dyne fiber was placed onto each of the braiding machine's 64 spools for a total of 64 fibers in the braid. This was done in contrast to conventional methods in which single fibers would be bunched to form yarns and these yarns would be subsequently braided. Given the size of the synthetic ligament desired, it was thought such an approach was ideal. The machine was put through two cycles before an acrylic dowel was used to tease the newly formed braids to the apex

before tightening the newly woven layers. The resulting woven mesh was approximately 3-4mm in thickness and 2mm deep.

The junction between the bone (microspheres) and ligament (braided fibers) can be seen in the figure to the left (black box). To fuse the two interfaces together, the ends of the ligament fibers were immersed in a mixture of acetone and water at a 2:8 ratio. Additionally a solution of acetone in water (3:7 ratio) was added to the region of the microspheres to receive the ligament fibers. The two polymeric interfaces were placed in contact with each other and a heated metal probe was placed on the interface, essentially sintering the two interfaces and simultaneously accelerating the evaporation of the solvent. After this, spot checks were done to determine the extent of bonding, and in areas of poor bonding at the interface, the procedure was repeated.

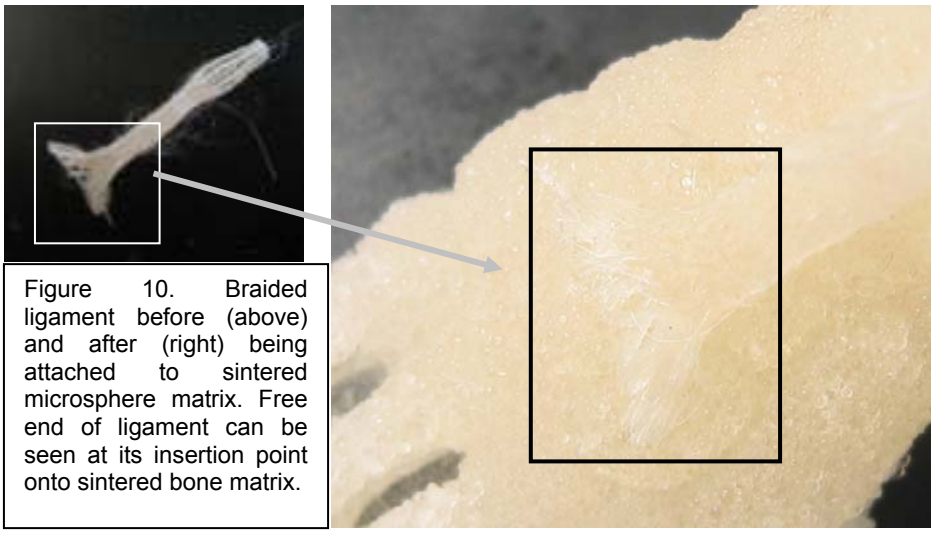

Figure 10. Braided ligament before (above) and after (right) being attached to sintered microsphere matrix. Free end of ligament can be seen at its insertion point onto sintered bone matrix.

Isolation of rabbit patellar tendon cells

The harvested patellar tendons from Fisher 344 rat were washed in sterile saline containing 2% penicillin/streptomycin and were cut into 1 mm sections. Tendon segments were incubated with 0.1% collagenase in low glucose Dulbecco's modified Eagle medium (DMEM; Invitrogen, Carlsbad, CA) for 1 hr at 37oC. Culture medium containing 10% fetal bovine serum, 1% penicillin/streptomycin and 0.25% ascorbic acid in DMEM was added and the solution was spun for 10 minutes at 3000g. The supernatant was removed and the pellet was washed two times with the above medium. The isolated cells and remaining tissue were plated in a 75-mm tissue culture flask and incubated (37°C, 5% CO2, 100% humidity) in supplemented DMEM culture medium. The medium was changed every two days until the cells became confluent. Cells were maintained at subconfluent level and passaged using trypsin/EDTA (GibcoBRL, Carlsbad, CA).

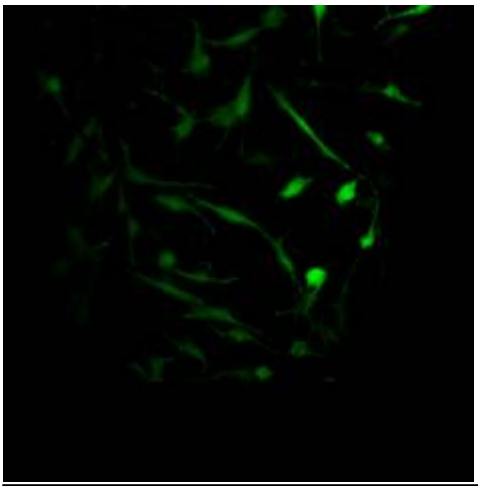

Figure 11. PTFs are visualized using Live/Dead Assay (Molecular Probes) at 14 days post-seeding (mag = 20x)

Preliminary studies were performed by culturing patellar tendon fibroblasts on PLAGA scaffolds prepared by electrospinning. Nanofiber scaffolds were prepared by electrospinning and seeded with primary patellar tendon fibroblasts (PTFs) harvested as described above. The scaffolds were sterilized and wetted in supplemented DMEM overnight prior to seeding at a density of 30,000 cells/cm^2. The seeded scaffolds were maintained in culture up to 28 days with media changes every 2 days. The cells attached to the scaffolds and displayed an elongated appearance. The cell processes are visible in the confocal image (see figure) taken at 14 days using 20x magnification. These processes are between the nanofibers that constitute the 3-D scaffold. Given the success of seeding these cells on nanofibers, it is anticipated that PTFs will perform equally well on braided ligaments. This will be evaluated in the near future.

QUARTER 3
The following milestones were identified within the third quarter:

In Vivo Studies
-Backpack model to evaluate vascularization of microsphere matrices with spun nanofibers
-μCT evaluation for ectopic bone formation in backpack model
-Time points: 3, 7, and 14 days

In Vivo Evaluation of Vascularization of Osteochondral Scaffolds

A dorsal skinfold window chamber was used as a model of angiogenesis and arteriogenesis to determine the vascularization potential of our multiphase, osteochondral scaffolds. In this preparation, a thin layer of fascia containing a robust microvascular bed was made visible through a glass window that was supported on the animal's back using two brackets that are fastened together (see figure 12). Under sterile conditions, the skin on the back was pulled into a fold with a clip. A circular incision, corresponding to the chamber diameter, was made in the skin on one side of the fold. The skin was then dissected free, leaving only fascia in the circle. One of the two chamber pieces was then placed on the skin fold. The biphasic scaffold, composed of both nanofibers (around the perimeter) and sintered microspheres (center) was placed in the window chamber (see figure 12). Following scaffold implantation, the second half of the window chamber was sutured to the first half through holes drilled in the chamber edges and the animal was allowed to recover. Periodically throughout healing the vasculature in and around the implant was visualized. To do this, the animal was anesthetized with inhaled isoflurane and placed on the stage of a Zeiss Axioskop, which was equipped with an x20 Achroplan and Plan Neofluar objectives.

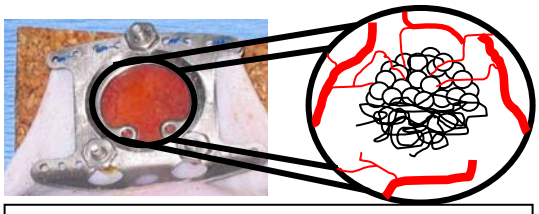

Figure 12. Backpack model to allow visualization of vascularization of osteochondral scaffolds.

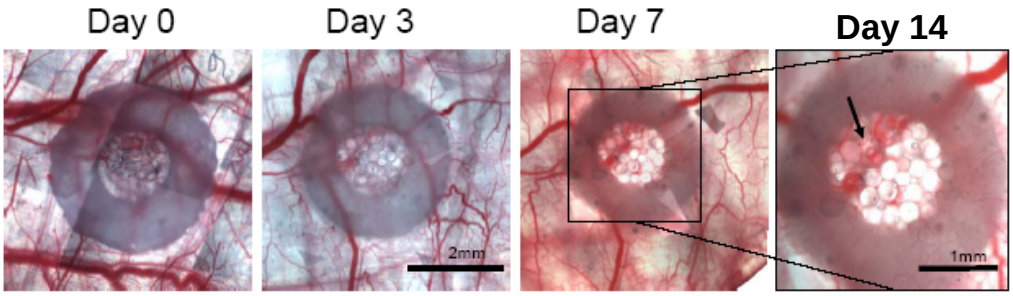

Figure 13. Representative images of the composite scaffold in the dorsal skinfold window chamber on days 0, 3, and 7 after implantation. Rightmost image highlights vascular ingrowth into the pores of the microspheres (denoted by arrow).

Results of the study are noted below. Periodic analysis (3, 7, and 14 days) indicated clear vascular ingrowth within the sintered microsphere matrices, which are designed to support vascularized bone growth, but no vascular ingrowth of spun nanofiber meshes, which are designed to support the largely avascular cartilage tissue. Vasculature was evident along the outer regions of the nanofiber mesh but was not seen to enter the pore structure of the mesh. The image at time point Day 0 below shows no evidence of vascular ingrowth in either the microsphere or the nanofiber portion of the scaffold, but at Day 14 there is clear evidence of a vessel growing along and into the microsphere matrix portion (black arrow). The path of the vessel extends across the inferior surface of the nanofiber mesh, towards the microspheres. The narrow pore structure of the nanofibers prevents vascularization of this portion but the relatively large pore structure of the sintered microsphere matrix encourages the ingrowth of vessels.

To further evaluate the ingrowth, or prevention of ingrowth, of vasculature into the matrix, tissue was fixed, sectioned, and stained using both cell and intracellular actin-specific stains.

Tissue Harvest, Fixation, Histology, and Immunohistochemistry

At the 14 day time point, mice were anesthetized with 2% isoflurane mixed with 1 ml/min O^2 and euthanized with an overdose of Nembutal administered intraperitoneally. Immediately, the chest cavity was opened and the vasculature was perfused with 10ml of 1x Tris-buffered saline plus 0.1mM $CaCl_2$ and 2% heparin via the right ventricle, followed by 10ml of 1x Tris-buffered saline plus 0.1mM $CaCl_2$ and 10ml 4% paraformaldehyde (PFA) for vessel fixation. During this time, 4% PFA was dripped onto the exposed vascular region of the window chamber. After perfusion and fixation, the window chamber tissue was excised using surgical microscissors and placed in a histological cassette in 4% PFA. Tissues were then embedded in paraffin, sectioned into 5μm slices and mounted onto glass slides.

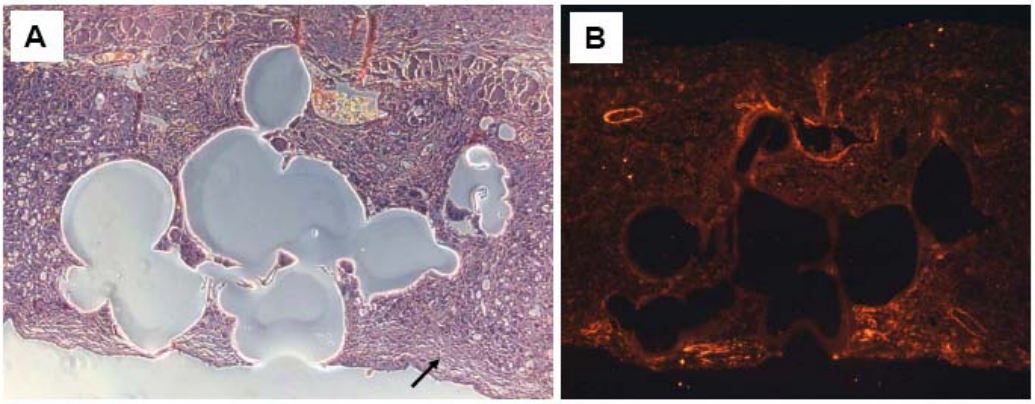

Figure 14. Representative images of a histological section through the scaffold in the dorsal window tissue. A) Tissue was stained for hematoxylin and eosin. Arrow points to location of nanofibers. B) Tissue was stained for smooth muscle α-actin, denoting the incorporation of smooth muscle cell-invested blood vessels. 40x.

Histological sections mounted on glass slides were de-paraffinized in two 10-minute washes of xylenes to remove the paraffin from the tissue sections and rehydrated using a graded series of ethanol solutions followed by two 5 minute washes of deionized water. Some samples were stained with hematoxylin and eosin (H&E) while remaining samples were immunolabeled for smooth muscle α-actin using CY3-conjugated monoclonal anti-SM α-actin (Sigma) diluted 1:500 in PBS/saponin/BSA (Chemicon). Slides were incubated with antibodies for approximately 15 hours at 4°C. Tissues were subsequently mounted using a 50:50 solution of PBS and glycerol. Immunolabeled histological tissue sections were imaged using a Axioskop 40 microscope (Carl Zeiss, Germany) equipped with fluorescence.

Figure 14 shows the results of histological analysis. Specifically, figure 14A shows the H&E stained cross-section of the implant, with the microsphere portion located in the center (empty spheres) and the nanofiber portion lateral to the microspheres (outlined in white). A blood vessel along the edge of the pore structure of the sintered microsphere matrix is clearly evident (white circle), further supporting light micrographs showing vessel ingrowth. No such images, however, were noted within the nanofiber mesh, confirming backpack model results that indicate all vasculature was confined to the exterior of the chondral portion of the biphasic implant. Actin staining (figure 14B) supports these findings by showing actin-positive staining (orange highlight) from smooth muscle cells co-localized to the vessel seen in figure 14A, but no staining within the nanofiber mesh, only confined to the inferior portion of the nanofibers. This suggests that vessels can grow along the nanofiber surface but are unable to penetrate its pore structure, as suggested by figure 13.

To evaluate the vasculature further, microCT imaging was combined with Microfil contrast agent.

Tissue Perfusion with MICROFIL®

Mice were anesthetized with 2% isoflurane mixed with 1 ml/min O_2 and euthanized with an overdose of Nembutal administered intraperitoneally. Immediately, the chest cavity was opened and the vasculature was perfused with 10ml of 1x Tris-buffered saline plus 0.1mM $CaCl_2$ and 2% heparin via

the right ventricle, followed by 10ml of 1x Tris-buffered saline plus 0.1mM $CaCl_2$. MICROFIL® was prepared according to product specifications (Flow Tech, Inc.). Briefly, 10 ml of diluent was mixed with 6 ml of MV compound and catalyzed with 5% (by volume) of MV Curing Agent. This solution was perfused through the right ventricle. After perfusion, the MICROFIL® was allowed to settle for 1 hours and then the window chamber tissue was excised using surgical microscissors and placed in a histological cassette in 4% PFA until microCT imaging.

MicroCT Imaging of Vessel Networks

High resolution scans of MICROFIL®-perfused backpack tissue was performed using a microcomputed tomography imaging system (vivaCT 40, Scanco Medical, Basserdorf, Switzerland). Control file parameters were set to high resolution 45 kVP. Two-dimensional slices were reconstructed into 3D volumes using the second evaluation program that designates two separate VOIs. Parameters for the solid VOI were set to 1.2 sigma, 2 support, and threshold from 144-1000. Parameters for the transparent VOI were set to 1.2 sigma, 2 support, and threshold from 30-144. The appropriate viewing orientation of the vessel networks within the backpack tissue was selected by rotation about the x-y-z axes. The reconstructed 3D image volume was exported as a .tif file.

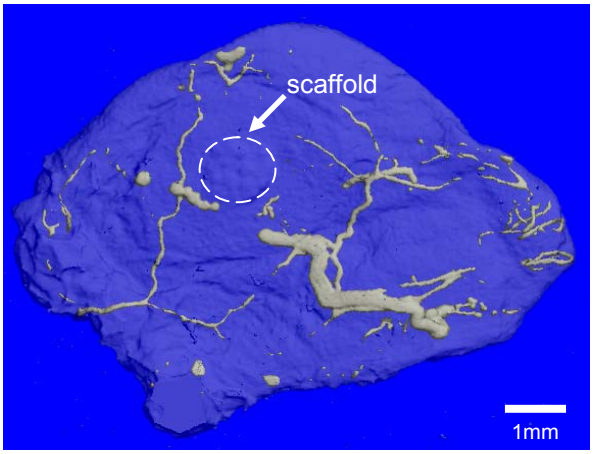

Figure 15. MicroCT representation of window chamber tissue. Vessels infused with microfil. Scaffold, with surrounding nanofibers, is highlighted.

Results from the microCT imaging show vessels positively localized to the perimeter of the microsphere scaffold (indicated within white circle in figure 15) but not clearly permeating the perimeter nanofiber portion of the scaffold, but also not permeating the more porous microsphere portion of the scaffold. This finding supports previous findings regarding nanofiber vascularization but confounds findings regarding microsphere vascularization. It is felt, however, that this is more a limitation of microCT resolution and Microfil® perfusion technique limitations, both of which are the subject of ongoing research.

QUARTER 4

The following milestones were identified within the fourth quarter:

To evaluate efficacy of the osteochondral grafts using an in vivo rat subcutaneous model

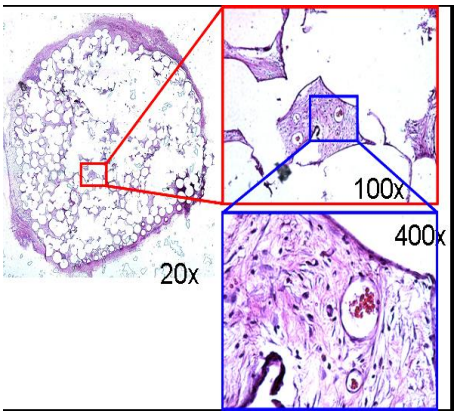

Figure 16A. Microsphere scaffold after 2 weeks of implantation. Cellular ingrowth is visible near the center of the implant, and evidence of vascularization is present.

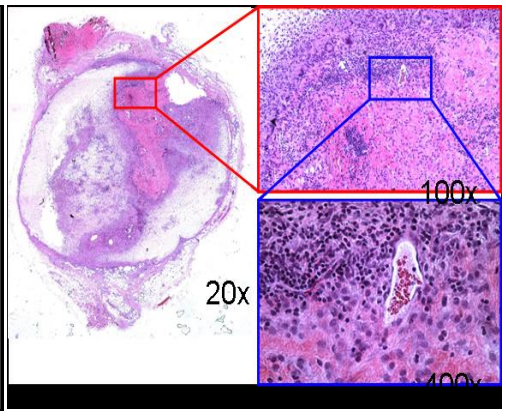

Figure 16B. Nanofiber scaffold after 2 weeks of implantation. Cellular ingrowth is visible near the center of the implant, suggesting cellular ingrowth.

Subcutaneous Implantation

Samples of microsphere and nanofiber matrix were inserted into subcutaneous pouches formed on the dorsum, lateral to the midline, of retired male breeder Sprague Dawley rats. Implants were allowed to heal for 2 (mirospheres and nanofibers) and 9 weeks (microsphere only), at which time they were removed, fixed in 10% formalin, sectioned and stained with Hematoxylin and Eosin to evaluate cellular infiltration and

foreign body response.

Figure 16A and 16B shows cellular response to implants after 2 weeks.

Figure 17 shows the microsphere matrix after 9 weeks of implantation. The 9 week implant, fashioned into a skeletal foot, was considerably larger than either the 2 or 4 week implant as the limits of cellular migration needed to be established. Figure 18 shows the construct prior to implantation (A), after nine weeks of healing but prior to removal (B), and after removal (C). Figure 18 shows histological sections indicating the cellular migration from the perimeter of the scaffold (A) almost through to its center (B). It is clear that after 9 weeks the tissue is able to migrate from the margins (figure 18) into the center (figure 19) of the implant, and that the implant maintains its shape. One challenge that exists with large scale implants, however, is the ability of cells to migrate throughout the scaffold structure. Figure 19 shows cells migrating as much as 6 mm from the perimeter to the center of the scaffold. There are areas of no cells within the implant, suggesting that complete infiltration has not occurred, but varying the pore size of the scaffold may correct this.

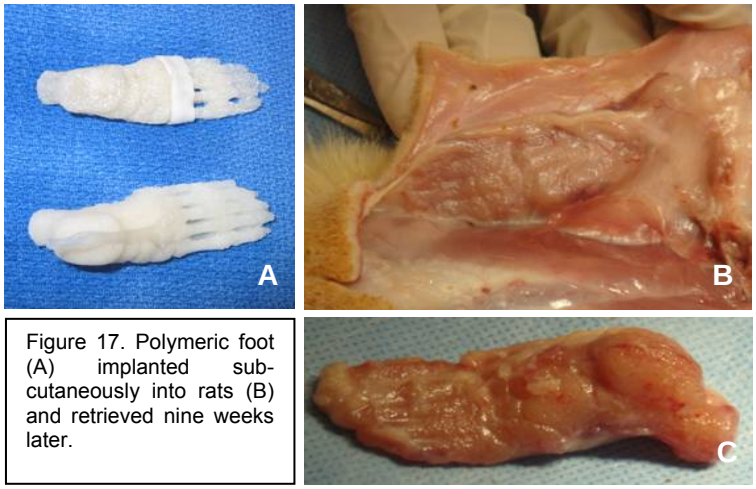

Figure 17. Polymeric foot (A) implanted sub-cutaneously into rats (B) and retrieved nine weeks later.

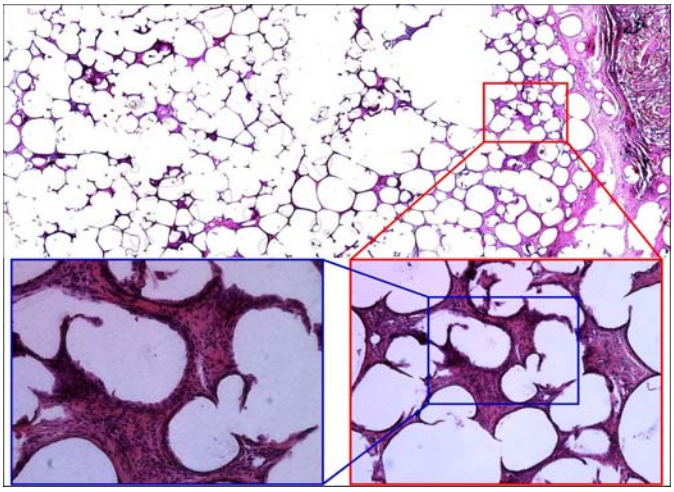

Figure 18. Histological sections of cell infiltration after 9 weeks of subcutaneous implantation. Cells are visible at the margins of the implant.

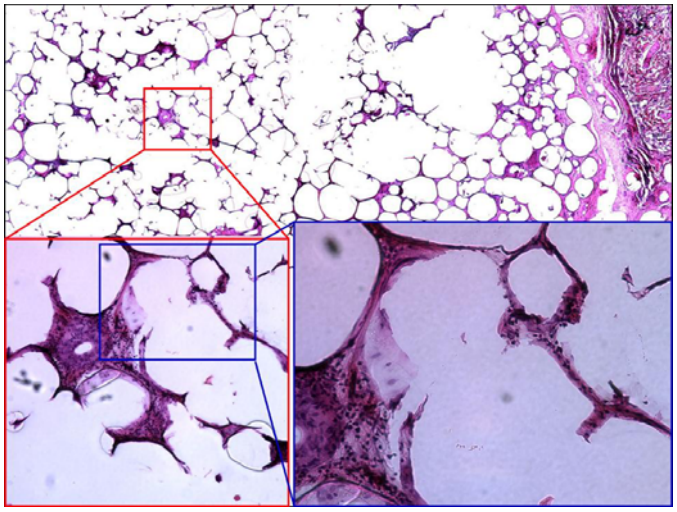

Figure 19. Histological sections of cell infiltration after 9 weeks of subcutaneous implantation. Cells are visible at the center of the implant, indicating good cellular infiltration.

KEY RESEARCH ACCOMPLISHMENTS

The following is a summary of the key research accomplishments of the work completed:

Quarter 1

- integration of nanofiber matrices with microsphere based matrices during nanofiber formation
- solvent bonding of nanofiber matrices with microsphere matrices
- Quantification of BMP-2 loading and delivery from microsphere matrices
- validation of HA incorporation to increase loading capacity of microsphere matrices
- Quantification of BSA release from nanofiber matrices
- Cellular evaluation of rabbit marrow stromal cells on microsphere matrices
- increased proliferation, ALP and OC synthesis over time on microsphere matrices
- Cellular evaluation of chondrocytes on

nanofiber matrices
- successful seeding and proliferation of chondrocytes on nanofiber scaffolds

Quarter 2
- synthesis of braided fiber ligament structure integrated with microsphere matrices
- seeding and visualization of proliferating rabbit patellar tendon cells on degradable matrices

Quarter 3
- in vivo evaluation of vascularization of nanofiber-microsphere matrix composite constructs
- evidence of vascular incorporation within microsphere matrix but not within nanofiber matrix
- evidence via both backpack model (in situ in vivo imaging) and histology

Quarter 4
-cells infiltrated large scale implants considerably well but not entirely
-limitations to complete infiltration may require variation in pore structure throughout implant

REPORTABLE OUTCOMES

In the one-year duration of this program, a supplementary grant proposal has been submitted to the National Institutes of Health based on preliminary findings resulting from this work. At this point a decision regarding funding has not been made.

CONCLUSION

The work completed in the initial year of this program has moved this team considerably closer to realizing its ultimate goal of limb regeneration. By building on the team's previous accomplishments, the tissue engineering of bone, ligament, and cartilage, and concentrating on the next hurdle towards total limb regeneration, the tissue engineering of the interface between musculoskeletal tissue types, crucial questions have been answered both in the materials science and the biological realm.

Important findings in the integration of scaffold structures have clarified future directions of scaffold fabrication. For instance, it was found that the direct synthesis of nanofibers on microsphere scaffolds for the osteochondral interface resulted in a very weak bond between the two interfaces and required an alternative strategy, the combination of heat, solvent, and pressure. These scaffolds were also found to have enhanced capacity as delivery vehicles when combined with calcium phosphate, the inorganic component of bone. Given these material property findings, a similar synthesis technique was successfully employed to form osteo-ligamentous interface scaffolds.

From the biological side, individual cell types corresponding to the type of tissue to be regenerated, ligament, bone, and cartilage, were all found to maintain phenotype when seeded on appropriate matrices. Vascularization was noted through the interior of the scaffold for bone repair but not through the synthetic cartilage scaffold which matches the natural state of each tissue. In vivo studies demonstrated good cellular infiltration throughout the bone scaffold but limited to no infiltration through the cartilage scaffold. This limited infiltration may require further study to determine the nature of in vivo tissue incorporation.

"So What" Section

The findings from this work have answered critical questions along the path from regenerating individual tissue types to regenerating intact limbs and organs that are comprised of many different tissue types. With scaffold-based tissue engineering as a platform, developing the interface between tissue types is a considerable challenge, and has been the focus of this research program. At the conclusion of this initial year of work novel and effective methods of building the interface and evaluating cellular behavior on either side of that interface has been completed. At the beginning of

the second year of this program, it will be possible to begin to engineer more extensive scaffolds that can incorporate additional scaffold structures both individually and together.

REFERENCES

None at this time.

APPENDICES

None at this time.

SUPPORTING DATA

None at this time.